chemistry

MDPI

Review

Is Aromatic Nitration Spin Density Driven?

Amedeo Capobianco, Alessandro Landi and Andrea Peluso *

Dipartimento di Chimica e Biologia "A. Zambelli", Università di Salerno, Via Giovanni Paolo II, 132, I-84084 Fisciano, SA, Italy; acapobianco@unisa.it (A.C.); alelandi1@unisa.it (A.L.)
* Correspondence: apeluso@unisa.it

Abstract: The mechanism of aromatic nitration is critically reviewed with particular emphasis on the paradox of the high positional selectivity of substitution in spite of low substrate selectivity. Early quantum chemical computations in the gas phase have suggested that the retention of positional selectivity at encounter-limited rates could be ascribed to the formation of a radical pair via an electron transfer step occurring before the formation of the Wheland intermediate, but calculations which account for the effects of solvent polarization and the presence of counterion do not support that point of view. Here we report a brief survey of the available experimental and theoretical data, adding a few more computations for better clarifying the role of electron transfer for regioselectivity.

Keywords: electrophilic substitution; aromatic nitration; electron transfer

check for updates

Citation: Capobianco, A.; Landi, A.; Peluso, A. Is Aromatic Nitration Spin Density Driven? *Chemistry* **2021**, *3*, 1286–1301. https://doi.org/10.3390/chemistry3040093

Academic Editor: Alessandro Ponti

Received: 20 October 2021
Accepted: 31 October 2021
Published: 4 November 2021

Publisher's Note: MDPI stays neutral with regard to jurisdictional claims in published maps and institutional affiliations.

Copyright: © 2021 by the authors. Licensee MDPI, Basel, Switzerland. This article is an open access article distributed under the terms and conditions of the Creative Commons Attribution (CC BY) license (https://creativecommons.org/licenses/by/4.0/).

1. Introduction

Electrophilic aromatic substitution has long been studied and, given the large amount of data reported in the literature, it represents a cornerstone in the field of mechanistic models of organic reactions, which excellent reviews and books have been dedicated to [1–4].

The lack of a kinetic hydrogen isotope effect and clearcut experimental evidence of the formation of ionic species have led to the well-accepted two-step mechanism, in which the attack of an electrophilic species to the aromatic substrate leads to the formation of an intermediate cyclohexadienyl cation [5], from which the reaction proceeds by fast proton abstraction.

Nitration has played a central role in the development of a mechanistic theory of aromatic reactivity [5–7]. Despite the great attention received and the huge body of experimental and theoretical data accumulated in many decades, many interesting facets of the nitration mechanism are far from being completely understood and the reaction mechanism is still the subject of active research [8]. Here, without the pretension of covering all the immense work done in the last seventy years, we present a critical review of both experimental and theoretical works related to aromatic nitration which have accumulated in the last half-century. We pose particular emphasis to the possible chemico-physical factors which make it possible that a very fast reaction can exhibit regioselectivity and add a few more computations aimed at better understanding the role of solvent in liquid-phase nitration.

2. Experimental Works

In the case of aromatic nitration, Ingold's pioneering work has shown that in reaction media composed of nitric acid (in acetic anhydride or nitromethane), the nitrating agent is the highly reactive nitronium ion and proposed the usual two-step mechanism with the formation of the Wheland intermediate (Scheme 1).

As nitrations of benzene and toluene were too fast to measure their absolute rates, Ingold developed the well-known competitive method in which only rate constant ratios

of different substrates were determined. It was found that in the above conditions toluene reacts significantly faster than benzene, with $k_T/k_B \approx 20$.

$$HNO_3 + HA \longrightarrow NO_2^+ + H_2O + A^-$$
$$NO_2^+ + ArH \longrightarrow ArHNO_2^+ \xrightarrow{A^-} HA + ArNO_2$$

Scheme 1. The mechanism proposed by Ingold.

Although Ingold's two-step nitration mechanism is still reported in most organic chemistry textbooks, kinetics measurements carried out in the early seventies by Schofield and Olah clearly showed that aromatic nitration deserved more attention, the extant mechanism being too simple to account for the observed kinetics. Schofield's group studied the nitration of several aromatic species using nitric acid in acidic media (sulphuric and perchloric acids). They found that the rates of nitration of aromatics more reactive than benzene reach a limit, which for alkylbenzenes is already achieved when two methyl groups are present, and concluded that for those more reactive aromatic substrates the nitration rate is encounter-limited [7,9]. In order to account for the observed kinetics, they proposed a three-step mechanism, see Scheme 2, in which the nitronium ion and the aromatic substrate form an adduct, an encounter pair (e.p.), which then leads to the formation of the Wheland intermediate.

$$HNO_3 + H^+ \underset{k_2}{\overset{k_1}{\rightleftharpoons}} NO_2^+ + H_2O$$
$$NO_2^+ + ArH \underset{k_4}{\overset{k_3}{\rightleftharpoons}} \text{e.p.}$$
$$\text{e.p.} \xrightarrow{k_5} \text{Products}$$

Scheme 2. The mechanism proposed by Schoefield.

The three step mechanism successfully explained kinetic data; indeed steady-state approximation to the reactions of Scheme 2 leads to the following expression for the observed second-order rate constant in terms of the ratio of the equilibrium concentration of NO_2^+ to the stoichiometric concentration of HNO_3:

$$k_{obs} = \frac{[NO_2^+]}{[HNO_3]} \frac{k_3 k_5}{k_5 + k_4},$$

with $k_{obs} = \text{rate}/[ArH][HNO_3]$. For reactive substrate, k_3 is much larger than k_2 and reaction rates depend only on the rate of formation of the intermediate species X, in agreement with experimental observations [9].

The necessity of a third step also arises from Olah's work, in which different reaction conditions for nitration were used. Olah and Kuhn developed efficient aromatic nitration by using stable nitronium salts, such as NO_2BF_4 and NO_2PF_6 [10]. Additionally, in that case, the reaction was revealed to be so fast to prevent the determination of absolute rate constants; the use of a competitive method for benzene and toluene substrates led to a ratio of rate constants $k_T/k_B \approx 2$, but the high positional selectivity for nitrotoluene, with the ortho and para carbons more reactive than meta one (ortho:meta:para = 66:3:31) was still observed. Those puzzling results led to the paradoxical conclusion that the meta carbons of toluene are sevenfold less reactive than benzene carbon. Using Olah's words, that observation is "inconsistent with any mechanism in which the individual nuclear positions compete for the reagent". Olah thus proposed that the first reaction step consists of the formation of a weakly bound π complex between the two molecular moieties, involving low, nonspecific, attractive interaction, which is responsible for substrate selectivity. The second faster step leads to the Wheland intermediate and accounts for positional selectivity, see Scheme 2.

Olah's argumentation was criticized [11,12]: The competitive method was considered inappropriate because the high reactivity of nitronium salts could not allow differentiation between the rates of different substrates; in other words, the low substrate selectivity could

be simply the consequence that reaction occurs before uniform mixing of the reagents is achieved. Olah responded to this criticism by showing that competitive experiments carried out varying the toluene/benzene mole ratio from 1:10 to 10:1 led to no significant changes in either positional or substrate selectivities [12], and concluded that the above results are not an experimental artifact but represent a new and important phenomenon, i.e., an electrophilic aromatic substitution displaying low substrate but at the same time high positional selectivity. That unusual property, common to several highly exothermic electrophilic aromatic substitutions in different reaction conditions, could be explained by postulating that the reaction proceeds via the formation of an intermediate species, i.e., the step determining substrate selectivity, followed by the formation of Wheland intermediate. The initial weakly bound intermediate species have been described variously as an encounter pair [9,13,14] with or without any significant interaction between reactants, a π complex [10,14,15], a charge transfer complex [16,17], and a radical ion pair, originated by an elementary electron transfer (ET) step from aromatics to NO_2^+ [18].

Gas-phase nitration was investigated by several authors; only charge transfer and oxygen atom transfer reactions:

$$NO_2^+ + ArH \rightarrow NO_2 + ArH^+$$
$$NO_2^+ + ArH \rightarrow NO\cdot + ArHO^+\cdot$$

were observed [19–22]. These studies were performed at low pressures in an ion cyclotron resonance spectrometer. The addition product $ArHNO_2^+$ was observed only by using $CH_2ONO_2^+$ as the nitrating species [23], but with that species the reaction exhibited different behavior: Aromatics containing electron withdrawing substituents appeared to be more reactive, in contrast to condensed phase reaction.

With the hope of providing mechanistic data which are not affected by the influence of the reaction medium but yet consistent with the results observed in solution, Cacace et al. found that using protonated methyl nitrate cation as nitrating species at atmospheric pressure, the reaction behaves as a typical electrophilic substitution of moderate selectivity, exhibiting several similarities with liquid-phase nitration. Even in the gas phase, positional selectivity is retained and, very interestingly, the nitration rate tends to a limiting value that cannot be increased by further enhancing the activation of the substrate, a behavior similar to the encounter-limited rates observed in solution [24].

The involvement of a radical ion pair in the mechanism of aromatic nitration, already proposed in the 1950s [16,25–27] was reconsidered by Perrin [18], on the basis of the gas-phase ionization potentials of reactive aromatics and NO_2 and electrochemical anodic half-wave potentials of NO_2 (1.82 V vs. Ag | 0.01 M $AgClO_4$ in CH_3CN) and of several reactive aromatics. The experimental anodic potentials showed that oxidation of naphthalene (1.34 V), anisole (1.4 V), mesitylene (1.62 V), and o-xylene (1.68 V) by NO_2^+ is thermodynamically favored for all the aromatics more reactive than toluene ($V_{ox} = 1.9$ V), even in a polar solvent such as acetonitrile. According to Perrin, an ET step in the reaction mechanism could solve the problem posed by the consideration that, if the attacking species were the highly reactive nitronium ion, there should be no intramolecular selectivity. Indeed the attacking species would no longer be the nitronium ion but the radical $NO_2^{\cdot}$, the latter being compatible with intramolecular selectivity, since the formation of the Wheland intermediate is necessarily a spin-density driven reaction.

Both the experimental and theoretical pieces of evidence provided by Perrin have been criticized [28], but the possible involvement of an ET step in the mechanism of aromatic nitration began to gain acceptance among organic chemists.

To better substantiate the hypothesis that a single electron transfer (SET) step could be of relevance in the mechanism of aromatic nitration, it would be important to assess whether the radical pair can actually lead to the Wheland intermediate and then to nitration products with the same isomer distributions commonly observed in conventional aromatic nitrations. Kochi and coworkers analyzed this important point [29,30]; because of the transitory character of the radical pair $(ArH^+\cdot):(NO_2\cdot)$, they used time-dependent spectroscopy

with picosecond time resolution to catch the possible formation of the ArH^+:NO_2 complex and to trace its time evolution [31]. It was well known that NO_2^+ and other nitronium carrier species are all electron-deficient and thus able to form electron donor–acceptor (EDA) complexes with different types of electron-rich donors, including aromatic hydrocarbons [32]. Those EDA complexes, often denoted as charge-transfer (CT) complexes, exhibit a significant red shift of their absorption band with respect to those of the parent species. That shift is thus assigned to an intermolecular absorption band due to promotion to an electronic state in which an electron is transferred from the donor to the acceptor [33].

Kochi et al. have shown that various ArH:NO_2 complexes can be thermally or photochemically activated toward nitration of the aromatic substrate. For instance, mixing N-nitropyridium cation ($PyNO_2^+$) to naphthalene in acetonitrile slowly leads to a mixture of 1- and 2-nitronaphthalene in excellent yields [34]. The same isomeric mixture is obtained when the yellow solution is initially cooled down to −40 °C, which inhibits the thermal nitration, and irradiated at the absorption wavelength of the CT complex [31]. Furthermore, time-resolved absorption spectra of the hexamethylbenzene EDA complex with tetranitromethane, recorded at different delay times after irradiation at the wavelength where the CT absorption occurs, yielded signals which were coherent with those observed in the absorption spectra of hexamethylbenzene cation, detected by spectroelectrochemical measurements, and of $C(NO_2)_3^-$ anion obtained from salt [35]. Noteworthy, the observed regiospecificity of the photoreaction is substantially indistinguishable from that obtained under conventional electrophilic conditions [31], and the byproducts are the same as those previously reported in the electrophilic nitration with nitric acid [36].

More recently, gas-phase mass spectrometric studies were performed for the reaction of the naked NO_2^+ and monosolvated ($CH_3NO_2{\cdot}NO_2^+$) nitronium ion with several monosubstituted aromatic compounds [37]. The naked nitronium ion reacts with benzene yielding exclusively the benzene cation. The adduct with m/z ratio corresponding to the Wheland intermediate was not observed, possibly because the formation of the Wheland intermediate is highly exothermic, being thus formed in highly excited vibrational states which, in the gas-phase, promote its fast dissociation in the ET products. A minor product at $m/z = 66$, diagnostic of the oxygen transfer reaction being produced after CO dissociation of the phenol cation, was also observed [19–22,38]. When gas-phase nitration of benzene is carried out with the nitronium ion carrier $CH_3NO_2{\cdot}NO_2^+$ the adduct with m/z ratio of the Wheland intermediate was clearly observed. Interestingly, the yields of such adduct decrease for aromatics more reactive than benzene (toluene and anisole); that is somewhat in contrast with what should be expected for the polar mechanism and more in line with the SET mechanism. Furthermore, for aromatics less reactive than benzene (nitrobenzene) nitration by $CH_3NO_2{\cdot}NO_2^+$ yields only the $PhNO_2NO_2^+$ adduct, without any evidence of the electron transfer reaction. Finally, Esteves et al. also showed that $CH_3NO_2{\cdot}NO_2^+$ reacts with halobenzene in a way which is consistent with the single electron transfer mechanism: while fluorobenzene and chlorobenzene form detectable amounts of the $PhXNO_2^+$ as well as the corresponding ionized halophenols, bromobenzene and iodobenzene, which have a lower ionization potentials, yield only the $PhX^+{\cdot}$ radical cation [37].

Very recently, an efficient system for the nitration of arenes at room temperature which allows for the observation of a π complex intermediate has been reported. That system consists of an equivalent of nitric acid in 1,1,1,3,3,3-hexafluoroisopropanol (HFIP). The π complex intermediate of an arene with a nitronium ion stabilized by HFIP can be directly observed by UV-vis spectra, as also supported by theoretical calculations [39].

3. Theoretical Works

Apart from considerations suggested by charge density computations and a few semiempirical calculations [40], to our knowledge, the first theoretical analysis of the mechanism of aromatic nitration was provided by Politzer and coworkers [41] who carried out *ab initio* SCF calculations, with a minimal basis set, of some intermediate species which could be formed in the reaction of benzene and toluene with a nitronium ion. Upon the

assumption that the reacting species is the free NO_2^+ ion, calculations showed that the rigid (both reactants restricted to their equilibrium ground-state geometries) approach of NO_2^+ to the aromatic molecule leads to the formation of a weakly bound π complex among the species, in which the positive ion is approximately parallel to the aromatic ring and roughly 2.8 Å above it, in a region where the nitronium ion experiences a negative electrostatic potential. The computed stabilization energies were -6.0 and -7.5 kcal/mol for benzene and toluene, respectively. For shorter distances, full optimizations of the whole systems lead to strongly bound complexes (the σ complex) with stabilization energies of -76 kcal/mol for benzene-NO_2^+ and -87 kcal/mol for toluene-NO_2^+. Only the weak π complex and the strongly bound σ complex were analyzed.

A few years later, Szabo and coworkers reported a computational analysis of the reaction profiles for aromatic nitrations [42]. Stationary points were located and characterized at the *ab initio* HF/3-21G level. Single point MP4(DQ)/3-21G calculations were carried out to evaluate the correlation energy correction for the activation barrier heights. The unsolvated nitronium ion reacts with benzene to give the Wheland intermediate without an energy barrier, but the protonated methyl nitrate, used by Cacace et al. in their gas-phase studies, reacts with aromatics to give an activation barrier which is substituent dependent and also depends on the solvating species.

The results of Szabo et al. were extremely intriguing; the authors interpreted them assessing that in the conventional solution nitration the nitronium ion has to overcome a desolvation barrier, a term coined by Dewar for denoting entirely solvent-related activation barriers without any contribution due to formation or breaking of chemical bonds [43]. However, they also argued that regioselectivity is not determined by the desolvation barrier, but rather by bifurcation points along the paths leading to different Wheland intermediates, the question concerning the origin of such bifurcation points being still unsettled. Peluso and Del Re tried to answer that point by performing theoretical computations specifically aimed at unraveling the possible role of a single electron transfer step in conventional nitration. Using multi-reference configuration interaction calculations with a small basis set and neglecting solvent effects, they analyzed the path corresponding to the rigid approach of the two moieties, using both the equilibrium geometries of neutral aromatics and the nitronium ion and those of the aromatic cation and neutral NO_2. They considered a limited number of approaching paths and found that in most cases the latter situation is energetically preferred with respect to the former [44]. That was not a surprising result, in view of the similar gas-phase ionization potentials of NO_2 and benzene and toluene. The most interesting point was that the energy barrier for the single electron transfer process was predicted to be much lower than it was believed from simple molecular mechanics calculations [44,45]. In a subsequent paper, Peluso and coworkers found for toluene nitration a conical intersection (CI) between the potential energy surfaces of the two electronic states located at ca. 3 kcal/mol above the energy of the reactants accommodated in a weakly bound π complex [45]. According to Peluso's computations, the electron transfer step is significantly exothermic and fast, occurring on timescales of a few picoseconds, independently of the approaching direction. Since internal conversion is usually very rapid, the rate-determining step could take place on the potential energy surface of the final state, thus accounting for regioselectivity. Instead, trapping of the reactants in the lowest energy state will make each collision effective for the reaction, thus accounting for the low substrate selectivity. That would explain why for aromatics more reactive than toluene the nitration rate is encounter-limited: the SET step acts as an harpoon [46], trapping reactants in electronic states which can mainly evolve toward nitration products or byproducts. Each collision thus becomes effective, even though the radical pair will take time to evolve in the Wheland intermediate. Furthermore, the high regioselectivity is also explained, because the formation of nitration products is spin density driven [44,45].

The paper by Peluso and Del Re stimulated a renewed interest toward the mechanism of aromatic nitration. Olah and coworkers published a paper entitled "Unified Mechanistic Concept of Electrophilic Aromatic Nitration: Convergence of Computational Results

and Experimental Data" [47] in which they revisited the mechanism of aromatic nitration proposing the involvement of three different intermediates along the reaction path: (i) an unoriented π complex or EDA complex, which is responsible for the low substrate selectivity in nitration with nitronium salts and of the observed oxygen transfer reactions in the gas phase; (ii) a SET complex, i.e., a radical pair consisting of an aromatic cation and neutral $NO_2\cdot$; (iii) an arenium ion, i.e., the Wheland intermediate. The involvement of radical pair intermediate was also verified by calculations carried out at the multi-configurational SCF (CASSCF) level, which is the most appropriate approach for handling such complex cases.

The introduction of three well-separated intermediates in the mechanism of aromatic nitration unify previous mechanistic proposals based both on experimental or theoretical evidence: Indeed, the initial interaction of benzene with a nitronium cation could either involve a SET or a π complex, both intermediates being minima on the potential energy surface; the preferential involvement of the one over the other will depend on several factors, including the nature of the aromatic species, especially its oxidation potential, the solvent, and reaction conditions.

The results presented by Olah et al. were also fully consistent with the mechanistic model proposed by Kochi [29,30,48], involving a metastable charge-transfer complex as the precursor to electrophilic aromatic substitution reactions. Indeed, light absorption used by Kochi to induce aromatic nitration is nothing else than an alternative way for passing from the π complex to the SET one, when thermal activation is precluded.

A further confirmation that a single electron transfer step is occurring in aromatic nitrations before the formation of the Wheland intermediate was provided by a theoretical paper by Kochi, Head-Gordon, and coworkers [48]. Based on the more sophisticated coupled-cluster methodology, that study evidenced the existence of two quasi-degenerate nuclear configurations in the region of noncovalently bonded reactants. The presence of two minimum energy structures bears a strong resemblance to the adiabatic electron-transfer surfaces of the Marcus–Hush theory [48–50], and is also very similar to the results of Peluso for toluene nitration [44].

An interesting generalization of Peluso and Del Re arguments to the whole class of the electrophilic aromatic substitution (EAS) was provided by Zilberg and Haas [51]. They advanced the hypothesis that for more reactive aromatic substrates, excited electronic states can be involved in the reaction mechanism, even in the absence of light. Indeed, energetic considerations regarding the ionization potentials of the electrophilic agents and aromatic substrates suggest that in the gas phase the reactants could be found in an electronically excited state, while products are formed in the ground state so that a crossing between electronic states must necessarily occur along the reaction path. In other cases, for aromatics with higher ionization potential or even for higher SET reorganization energies, the reaction starts on the ground state. Thus EAS can be divided into two classes, depending on whether the reaction begins on an excited electronic state or on the ground electronic state. In the former case, the reaction proceeds essentially without any energy barrier either by two electron processes (polar mechanism) or by a SET, depending on the character of the conical intersection. The second class of EAS reactions occurs exclusively on the ground electronic state and a π complex is initially formed. In some cases, as for instance benzene nitration, the SET process competes with the polar reaction path. In solution, EAS reactions could prevalently occur on the ground state, because of the preferential solvation of the electrophilic species.

Esteves and coworkers [37] carried out accurate *ab initio* computations to interpret their results concerning gas-phase nitration, see the previous paragraph. They found that the SET mechanism is preferentially involved for substituted aromatics with ortho/para directing groups, whereas, for deactivating groups, for which substitution at the meta position is mainly observed, the classical polar Ingold–Hughes mechanism is preferred. They proposed that the SET and the classical polar Ingold–Hughes mechanism represent two competing mechanisms, the prevalence of either one of them depends on whether the aromatic compound is capable to transfer an electron to the nitronium ion.

Another interesting theoretical analysis of the nitration mechanism was provided by Lelj, MacLachlan et al. and concerned with the dinitration of 1,2 and 1,4-dialkoxybenzenes, which exhibit unusual regioselectivity. Their results show that the reaction mechanism is likely to involve a SET process. In the case of the former isomer, the regioselectivity is mainly determined by the symmetry of the HOMO of the aromatic moiety that defines the structure of the singly highest occupied molecular orbital (SHOMO) of the aromatic radical cation formed by the SET process. For the dinitration of 1,4-dialkoxybenzenes, DFT calculations indicated that the 2,3-dinitro and 2,5-dinitro products should both be formed and that the relative amounts should mostly be influenced by the solvent environment and may thus be altered depending on the solvent environment. Synthetic studies of the nitration of 1,4-dialkoxybenzene derivatives using different solvent conditions supported this conclusion and provided practical information for tuning the regioselectivity of the reaction [52].

More recently, the SET mechanism has been questioned by several authors, at least as concerns liquid-phase nitrations [53–55]. Parker and coworkers re-examined benzene nitration by nitronium ion in the gas phase using high-level *ab initio* computations (MP2/6-311++G**), posing particular emphasis in finding out continuous paths, in particular the intrinsic reaction path (IRC), which connects all the relative minimum energy structures predicted by computations through transition states. The analysis revealed the existence of intermediates and transition states which were not found in previous investigations. No nitration product derived from the radical pair $Ar^{+}\cdot NO_2\cdot$ was found, IRC analyses provided results in favor of the polar mechanism [53].

Similar conclusions were also reached by Galabov and Schaefer III, even though they were limited to nitration in mixed acid solutions. They carried out DFT/M06-2X computations both in the gas-phase and in the liquid phase, considering both bulk solvent effect and the explicit association of the electrophile with a single H_2SO_4 molecule. In the gas phase, population analysis predicts a large amount of electron transfer from benzene to the nitronium ion, whereas, in mixed acid solutions, when association with a counterion is considered, no appreciable charge transfer is predicted [54].

A very different point of view has been provided by Quinone and Singleton, who questioned both the importance of a SET intermediate and the involvement of transition states. Those authors carried out a thorough analysis of the ground state potential energy hypersurface for toluene nitration by NO_2BF_4 in dichloromethane and found that the regiochemistry of the reaction is accurately predicted only from trajectories in explicit solvent, while approaches based on transition state theory fail to account for selectivity. Computations predict that although no free-energy barrier is found on going from the encounter complex to the reaction products, yet the trajectories require a long time (of the order of ps) to descend an exoergonic slope. Regioselectivity is achieved only at almost the ending time of each trajectory. In order to understand something more on regioselectivity, trajectories were run for three simplified models: (*i*) without explicit solvent molecules; (*ii*) without explicit BF_4^- counterion; (*iii*) without both counterions and explicit solvent molecules. None of these simplified models yields accurate results, the impediments due to both solvent and counterion reorientations are indeed crucial for trajectories to achieve the right selectivity toward substitution positions [55].

4. The Rigid Approach of Reactants in Solution

Criticism of the involvement of a SET step in the mechanism of aromatic nitration mainly concerns the reaction in solution [54]. For better assessing the effect of solvent medium, herein we have carried out a few DFT computations aimed at understanding the relative energy positions of the two diabatic states which could be involved in the nitration mechanism, following very closely the approach of Peluso and Del Re and Zilberg and Haas [44,51] who unfortunately have limited their analyses to the gas phase. Indeed, in our opinion, the behavior of the system in the region of intermolecular distances short enough to allow for SET but not for the formation of a chemical bond between reactants is

crucial for a better understanding of the reaction mechanism. We have thus considered two sets of diabatic states possibly leading to a π complex. One, denoted by $|\mathrm{ArH}\cdots\mathrm{NO_2^+}\rangle$, approximately describes the interaction of the aromatic hydrocarbon ArH (ArH = benzene, toluene) with NO_2^+; the other, denoted by $|\mathrm{ArH^+}\cdots\mathrm{NO_2}\rangle$, describes the diradical pair state obtained by SET, where neutral NO_2 interacts with ionized ArH^+. The two diabatic states are defined by taking advantage of the very different equilibrium geometries of NO_2^+ and $NO_2\cdot$, the former being linear, the latter significantly bent. The very high reorganization energy characterizing the NO_2^+/NO_2 redox couple insures against the mixing of the two electronic states. Of course, those diabatic states have physical meaning only for weak interactions between the two molecules, and that is the meaning of dots in the ket symbols.

The benzene radical cation is characterized by two nearly degenerate states, usually termed as "compressed" $^2B_{2g}$, slightly more stable, and "elongated" $^2B_{3g}$, see [56–59]. Thus, two $|\mathrm{ArH^+}\cdots\mathrm{NO_2}\rangle$ states have been considered for benzene, herein denoted as $|{}^2\mathrm{B_{2g}}^+\cdots\mathrm{NO_2}\rangle$ and $|{}^2\mathrm{B_{3g}}^+\cdots\mathrm{NO_2}\rangle$. In order to be consistent with that notation, $|{}^1\mathrm{A_{1g}}\cdots\mathrm{NO_2^+}\rangle$ indicates the $|\mathrm{ArH}\cdots\mathrm{NO_2^+}\rangle$ state for benzene.

In the computations of the energy profiles for the approach of the two rigid reactants in the $|\mathrm{ArH^+}\cdots\mathrm{NO_2}\rangle$ and the $|\mathrm{ArH}\cdots\mathrm{NO_2^+}\rangle$ electronic states, different orientations indicated as A, B, C, and D in Figure 1 have been considered. The distance r between reactants has been varied from 2.15 up to 5.15 Å, in steps of 0.10 Å.

For each tested distance, the nature of the diabatic states (polar vs. diradical) was checked by inspection of the HOMO and LUMO Kohn–Sham orbitals and by atomic charges: For both benzene and toluene, the net charge of NO_2 remains close to one in all the points of the $|\mathrm{ArH}\cdots\mathrm{NO_2^+}\rangle$ profiles and close to zero for all the points of the $|\mathrm{ArH^+}\cdots\mathrm{NO_2}\rangle$ profiles (see the Supplementary Materials).

The relative stability of the diabatic states at infinite separation of monomers is dictated by the adiabatic ionization potentials of benzene, toluene, and NO_2. Predicted and experimentally available data are reported in Table 1. In pretty good agreement with their experimental counterpart, predicted ionization potentials of NO_2, benzene and toluene are consistent with a picture in which the $|\mathrm{ArH^+}\cdots\mathrm{NO_2}\rangle$ state is more stable than the $|\mathrm{ArH}\cdots\mathrm{NO_2^+}\rangle$ at infinite separation of monomers for benzene and a fortiori for toluene.

The energy profiles predicted for the gas phase by DFT computations for benzene are reported in Figure 2. For paths A and B, the polar state is favored only for distances within the range 2.6–3.6 Å, and it exhibits an absolute (within the rigid approach employed here) minimum at $R = 3.05$ Å, with interaction energies amounting to ca -3.5 kcal/mol for both arrangements. At shorter distances, the electron transfer from benzene to NO_2^+ is again favored, as testified by the $|{}^2\mathrm{B_{2g}}^+\cdots\mathrm{NO_2}\rangle$ and $|{}^2\mathrm{B_{3g}}^+\cdots\mathrm{NO_2}\rangle$ curves lying below $|{}^1\mathrm{A_{1g}}\cdots\mathrm{NO_2^+}\rangle$ (see also Tables S1 and S2 in the Supplementary Materials). Noteworthy, the interaction energy of the $|{}^1\mathrm{A_{1g}}\cdots\mathrm{NO_2^+}\rangle$ state is predicted to rise upon shortening the distance between NO_2 and benzene. Indeed, path A does not allow bonding interactions between the MOs of the two reactants, whereas arrangement B gives rises to an in-phase interaction between one of the occupied e_{1g} orbitals of benzene and an empty π MO of the nitronium ion [44,47].

Table 1. Predicted gas phase (ωB97XD/ma-TZVP) and experimental adiabatic ionization potentials (eV).

	DFT	DFT [a]	Exper.
NO_2	9.68	9.60	9.59 [b]
benzene [c]	9.29	–	9.24 [d]
toluene	8.60	8.65	8.83 [e]

[a] Without zero point vibrational energy (ZPVE) correction. [b] Ref. [60]. [c] Vertical ionization potentials; the predicted adiabatic ionization potentials are 9.05 and 9.12 (without ZPVE) eV. [d] Ref. [61]. [e] Ref. [62].

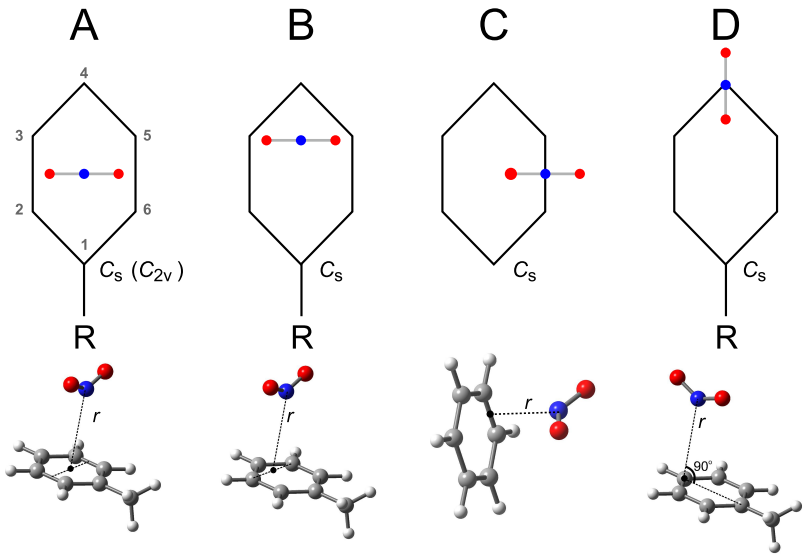


Figure 1. Illustrative pictures of the explored coordination paths. In path A, the projected direction of N–O bonds lies parallel to the line bisecting the bonds between ortho and meta C atoms of the aromatic ring, with N insisting perpendicularly over the geometric center of the ring; *r* denotes the distance between N and the center of the ring. Arrangement A assumes C_s (C_{2v}) symmetry for toluene (benzene). In path B, the projected direction of N–O bonds lies parallel to the line connecting C3 and C5, with N insisting perpendicularly over the center of that line; *r* denotes the distance between N and the midpoint of the C3–C5 line. In path C, the projected direction of N–O bonds lies parallel to the line bisecting one of the C-C bonds of the aromatic ring; for $^2B_{2g}$ ($^2B_{3g}$) states of benzene, the compressed (elongated) C-C bond has been chosen, with N insisting perpendicularly over the center of that bond; *r* denotes the distance between N and the center of the C-C bond. In path D, the projected direction of N–O bonds lies parallel to the line connecting the C bearing the R substituent and the C in para position, with N insisting perpendicularly over the carbon in para; *r* denotes the distance between N and the C atom in para position.

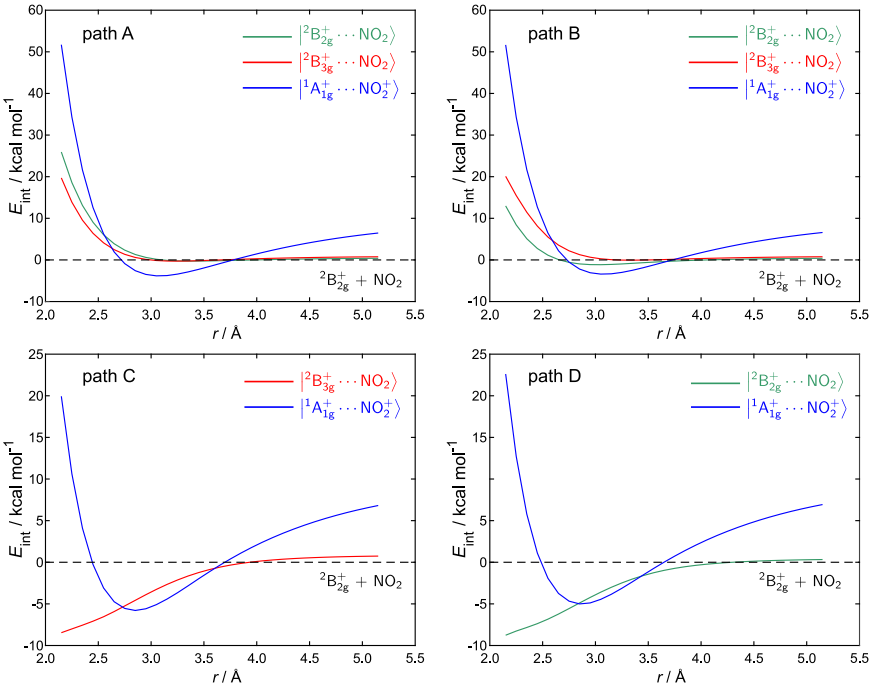


Figure 2. Predicted interaction energy of benzene/benzene$^+$ with NO_2^+/NO_2 in the gas phase as a function of the distance of the interacting units, oriented as in the paths A, B, C, and D of Figure 1.

The profiles of paths C and D are particularly interesting, because those orientations are known to yield stable π complexes with bent NO_2 coordinated to benzene at $r \approx 2$ Å (see Figure 2). Based on previous works by Olah and Parker [47,53], only the $|^2B_{3g}{}^+ \cdots NO_2\rangle$ ($|^2B_{2g}{}^+ \cdots NO_2\rangle$) state has been considered for path C (D), since it leads to a stable adduct with elongated (compressed) benzene. The potential energy profile for the rigid approach of reactants in the diabatic $|^2B_{3g}{}^+ \cdots NO_2\rangle$ electronic state of path C exhibits a monotone increase from 2.15 up to 5.15 Å. Instead, the interaction energy of the $|^1A_{1g} \cdots NO_2^+\rangle$ state exhibits a minimum at 2.85 Å (see also Tables S3 and S4 in the Supplementary Materials). However, that minimum lies ca. 3 kcal/mol above the $|^2B_{3g}{}^+ \cdots NO_2\rangle$ curve at 2.15 Å, which implies that the evolution of the π complex toward the reaction products can proceed via an electron transfer step from benzene to NO_2^+. Identical considerations also hold for path D, upon reversing the roles of $|^2B_{2g}{}^+ \cdots NO_2\rangle$ and $|^2B_{3g}{}^+ \cdots NO_2\rangle$.

The energy profiles for toluene, for which only paths A, B, and D have been considered, are reported in Figure 3. Due to the lower ionization potential of toluene, the $|ArH^+ \cdots NO_2\rangle$ state is always favored with respect to $|ArH \cdots NO_2^+\rangle$, whether or not the path yields a stable π complex, thus demonstrating that SET is likely to occur in the mechanism of gas-phase nitration of toluene (see also Tables S5–S7 in the Supplementary Materials).

Adiabatic ionization potentials (including ZPVE) in dichloromethane are predicted to be 6.91, 7.12, and 6.78 eV, for NO_2, benzene, and toluene, respectively, by PCM computations. Those results are in good agreement with the outcomes of previous electrochemical estimates, which found the oxidation potential of toluene higher by 0.1 V than that of NO_2 in acetonitrile [18]. In the light of the above potentials, SET should not result in an affordable process for benzene at infinite separation of reactants, but it is still possible for toluene. Without including ZPVE (in order to be consistent with the curve profiles), adiabatic ionization potentials are estimated to be 6.82 eV for both toluene and NO_2, and 7.18 eV for benzene.

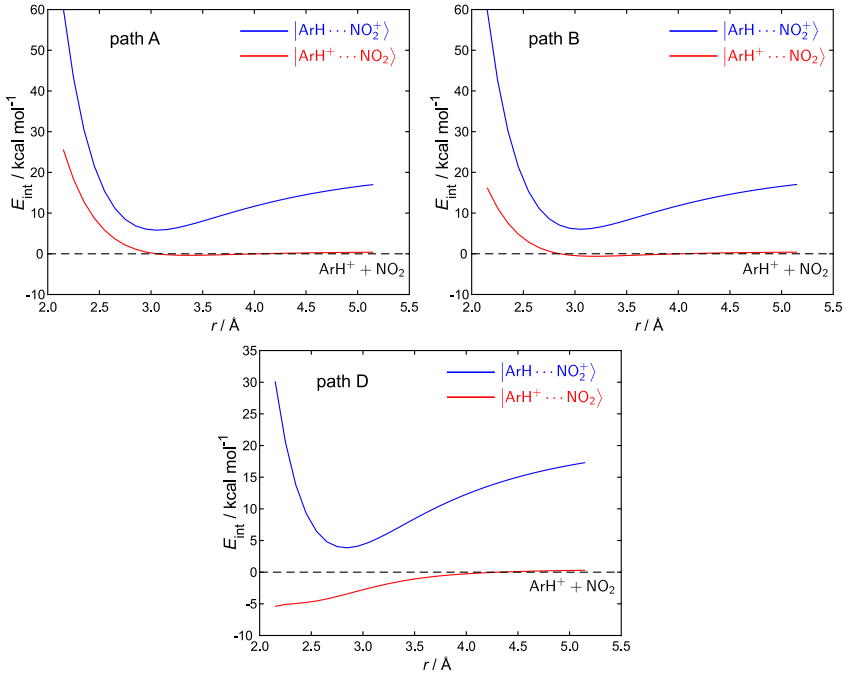


Figure 3. Predicted interaction energy of toluene/toluene$^+$ with NO_2^+/NO_2 in the gas phase as a function of the distance of the interacting units, oriented as in the paths A, B, and D of Figure 1.

The energy profiles for benzene in dichloromethane are reported in Figure 4.

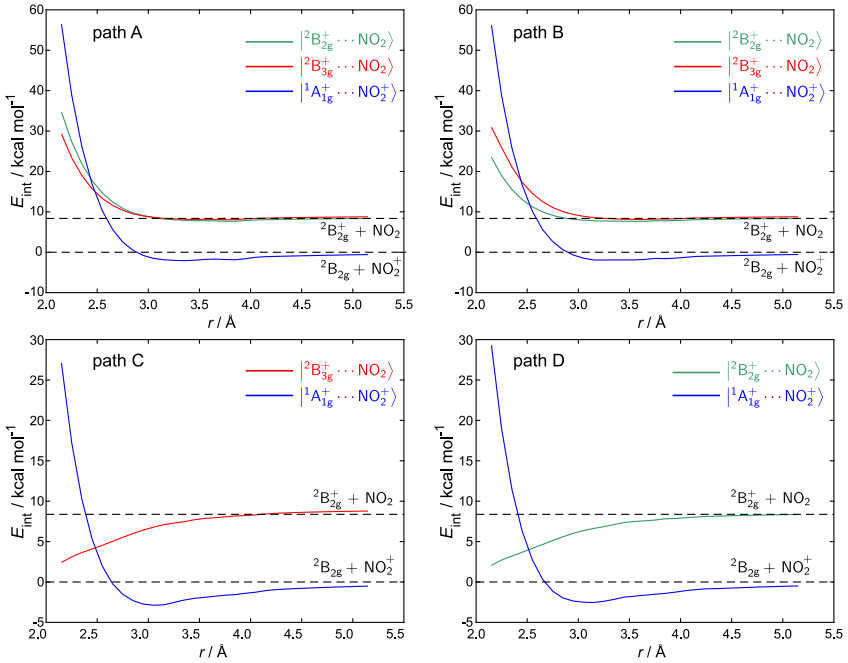


Figure 4. Predicted interaction energy of benzene/benzene$^+$ with NO_2^+/NO_2 in dichloromethane as a function of the distance of the interacting units, oriented as in the paths A, B, C, and D of Figure 1.

Independently of the explored path, the polar state $|^1A_{1g}\cdots NO_2^+\rangle$ remains stable up to ca. 2.5 Å. At shorter distances, the SET is predicted to also occur in solution. Indeed, for both paths A/B, which do not give rise to stable π complexes, and C/D giving rise to stable complexes, the curves corresponding to the $|ArH^+\cdots NO_2\rangle$ states systematically fall below the one of the $|ArH\cdots NO_2^+\rangle$ states (see also Tables S8–S11 in the Supplementary Materials).

Energy profiles for toluene in dichloromethane are reported in Figure 5.

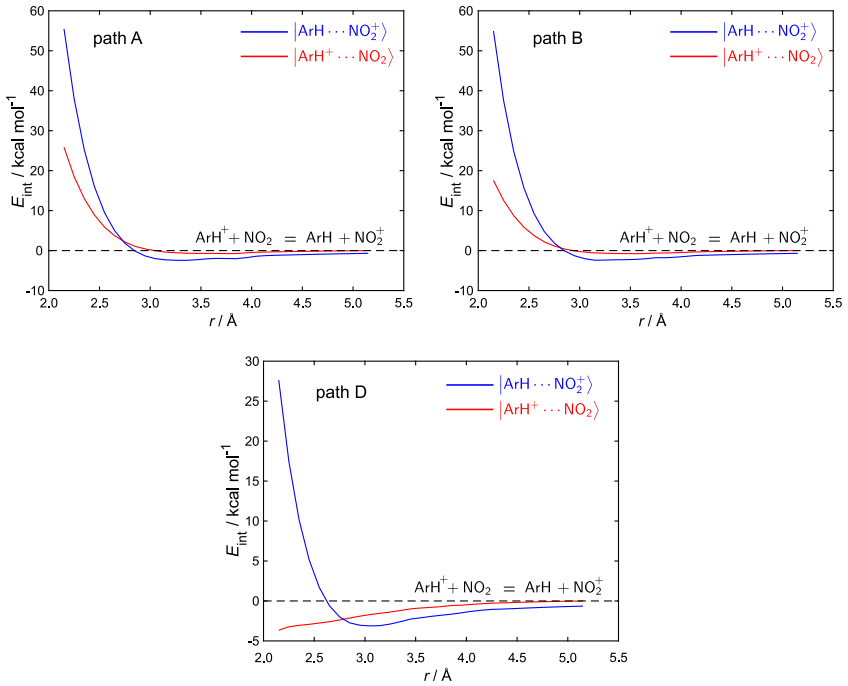


Figure 5. Predicted interaction energy of toluene/toluene$^+$ with NO_2^+/NO_2 in dichloromethane as a function of the distance of the interacting units, oriented as in the paths A, B, and D of Figure 1.

At variance with benzene, the $|\mathrm{ArH}^+ \cdots \mathrm{NO_2}\rangle$ state turns out to be disfavored with respect to $|\mathrm{ArH} \cdots \mathrm{NO_2^+}\rangle$ to a very small extent. Independent of the path, energy differences lower than 1 kcal/mol are predicted for the different states at $r > 3.10$ Å. The $|\mathrm{ArH} \cdots \mathrm{NO_2^+}\rangle$ state exhibits a minimum at 3.05 Å for all the explored paths, where the $|\mathrm{ArH}^+ \cdots \mathrm{NO_2}\rangle$ state lies ca. 1.5 kcal/mol higher, with the $|\mathrm{ArH}^+ \cdots \mathrm{NO_2}\rangle$ state becoming favorite at $r \leq 2.8$ Å (see also Tables S12–S14 in the Supplementary Materials).

The results reported above suggest a few brief considerations. Path A and path B are always dissociative; independently of the electronic state, high energy barriers are predicted along these paths for reaching the region of the products. That could partially explain why nitration does not occur in the gas phase at low pressure; indeed paths A and B are statistically more representative of a molecular collision between "traveling" species, i.e., species possessing non-negligible kinetic energy, for which a minimum energy path toward reaction products has little physical meaning. Upon mixing reactants, collisions occur when they are in the $|\mathrm{ArH} \cdots \mathrm{NO_2^+}\rangle$ state and lead the system in a weakly bound π system which can only evolve toward the electron transfer products. No significant attractive interaction is predicted for the SET products, so that further collisions will not be reactive at low pressure. Paths C and D are instead representative of collisions in which the encounter pair has a longer lifetime, being thus able to explore a larger region of the potential energy surface. In that case, reactants could be able to find reactive channels which lead to products. Our analysis, although being very limited for providing conclusive assessments, suggests that in those cases a SET step is very probable, since the potential energy profile for reactants approach in the $|\mathrm{ArH} \cdots \mathrm{NO_2^+}\rangle$ state is repulsive, while that corresponding to the $|\mathrm{ArH}^+ \cdots \mathrm{NO_2}\rangle$ state is instead attractive. Those preliminary considerations need further investigations for being confirmed on a statistical ground, the number of paths considered here being too limited.

As concerns the reaction in the liquid phase, our results show some interesting features, which are worthy of future consideration. For benzene, the $|\mathrm{ArH} \cdots \mathrm{NO_2^+}\rangle$ state lies at lower energy than the $|\mathrm{ArH}^+ \cdots \mathrm{NO_2}\rangle$ one for long intermolecular distances, the energy crossing of the two states occurring at $r \approx 2.5$ Å, independently of the path. At such short intermolecular distances it is somewhat risky to claim that SET is a distinctive reaction step of the nitration reaction. Our results show that in toluene the situation is similar but the crossing point between the two potential energy profiles occurs now at $r \approx 2.8$ Å. For substrates more reactive than toluene it can be envisioned that SET can take place at still longer intermolecular distances, so that it becomes the first step in the mechanism of aromatic nitration in the liquid phase, of course after the formation of free nitronium ion. The SET step can easily account for the encounter-limited behavior exhibited by more reactive aromatic substrates, inasmuch as the formation of the radical pair can be fast enough to compete for dissociation of the encounter pair and, being significantly exoergonic, can trap reactants together, making each collision effective for the reaction. The SET step thus will act as a harpoon, very similar to what occurs in the reaction of K with methyl iodide.

5. Concluding Remarks

Aromatic nitration is a fast reaction characterized by a clearcut intramolecular selectivity. These somewhat contrasting features can be accommodated together into a kinetic law by assuming the formation of an intermediate species, which is responsible for the observed regioselectivity. The nature of the intermediate has long been debated, none of the proposed species comfortably fitting all observations. Theoretical calculations also provided discordant answers, evidence in favor of the formation of a radical pair, suggested by the first quantum mechanical computations, has been later questioned at least as concerns the reaction in the liquid phase, so that a conclusive assessment has not been reached yet. Here, we have shown that an electron transfer step is conceivable in the liquid phase too, but the present computations have only addressed the rigid approach of the two reactants in a limited region of the potential energy surfaces which prevents the formation

of chemical bonds. Further studies are therefore needed for a deeper understanding of the chemico-physical factors governing regioselectivity in aromatic nitration. That task is not easy: Two electronic states have necessarily to be taken into consideration during the whole course of the reaction, so that useful tools usually employed for analyzing the course of chemical reactions, such as the minimum energy path and the location of transition states, could become misleading. Notwithstanding, we believe that a traditional reaction mechanism of aromatic nitration in terms of identification of all critical structures and recognition of the factors that affect reactivity can be found, without resorting to provide ensembles of trajectories describing atomistic motions during the course of the reaction, in which chemical information may be lost.

6. Computational Details

Geometry optimizations of the monomers in their neutral and positively charged states, as well as single point computations for the A-D paths of benzene and toluene, were carried out at the density functional level of theory (DFT) by using the ωB97X-D functional. The latter adds an empirical correction for dispersion energy to the ωB97X range separated hybrid functional, which recovers the exact $1/r$ asymptotic behavior of the exchange potential [63]. The ma-TZVP basis set, namely def2-TZVP augmented with s and p diffuse functions for nonhydrogen atoms was adopted throughout [64]. That basis set should ensure very low basis set superposition errors, achieving the same performances as more extended sets, see e.g., [65]. With the exception of geometry optimizations of NO_2, benzene, and toluene in their neutral state, the unrestricted formalism was used in all computations. It must be stressed that it is mandatory to employ the unrestricted formalism for the $\left|ArH^+ \cdots NO_2\right\rangle$ state, where NO_2 retains its bent configuration in computations carried out at the Hartree–Fock or Kohn–Sham DFT levels. Indeed, restricted SCF computations systematically suffer from external instability [66,67]. Furthermore, restricted SCF procedure is likely to not converge at all for monomer distances exceeding $\approx$ 3.5 Å in the case of benzene, that drawback being even more dramatic for toluene. Instead, the unrestricted solution was found to converge to the restricted one for all the points of the $\left|ArH \cdots NO_2^+\right\rangle$ state.

Atomic charges were computed by using the charge model 5 (CM5) modification of the Hirshfeld populations. However, very similar trends were also obtained by using different approaches such as natural atomic populations and ESP charges [68–70].

Computations including solvent (dichloromethane) effects were carried out by employing the polarizable continuum model (PCM) allowing for equilibrium solute–solvent interaction [71]. The geometry of the $^2B_{3g}$ state of ionized benzene was taken from [56] and used as such in all computations for both the gas and the solution phase. The predicted equilibrium geometry of toluene cation radical deviates from C_s symmetry to a very small extent, due to a slightly asymmetric torsion of the methyl group. Nevertheless, C_s symmetry has been imposed for toluene cation in single point computations of energy profiles, in order to preserve C_s symmetry for the orientations A, B, and D of Figure 1. That approximation does not result in appreciable errors, inasmuch as in toluene$^+$ the methyl group has been observed to undergo a nearly free rotation, whose torsional barrier is estimated to be just 16 cm^{-1} [62].

DFT computations were carried out by using the Gaussian package [72].

Supplementary Materials: The following are available at https://www.mdpi.com/article/10.3390/chemistry3040093/s1, Figures S1–S4: CM5 charges of the NO_2 moiety in $\left|ArH \cdots NO_2^+\right\rangle$ and $\left|ArH^+ \cdots NO_2\right\rangle$ diabatic states; Tables S1–S14: Critical points of the energy profiles; Cartesian coordinates of all the investigated systems with interacting units at $r = 3.05$ Å, for the A, B, C, and D paths.

Author Contributions: Conceptualization, A.P. and A.C.; funding acquisition, A.P. and A.C.; investigation, A.P., A.L., and A.C.; methodology, A.C. and A.P.; project administration and resources, A.C. and A.P.; software, A.C.; writing, A.C., A.L., and A.P. All authors have read and agreed to the published version of the manuscript.

Funding: This research was funded by the Università di Salerno, grants: FARB 2019 and FARB 2020.

Institutional Review Board Statement: Not applicable.

Informed Consent Statement: Not applicable.

Data Availability Statement: Not applicable.

Conflicts of Interest: The authors declare no conflict of interest.

References

1. Norman, R.O.C. *Electrophilic Substitution in Benzenoid Compounds*; Elsevier: New York, NY, USA, 1965.
2. Taylor, R. *Electrophilic Aromatic Substitution*; Wiley: New York, NY, USA, 1990.
3. Stuyver, T.; Danovich, D.; De Proft, F.; Shaik, S. Electrophilic Aromatic Substitution Reactions: Mechanistic Landscape, Electrostatic and Electric-Field Control of Reaction Rates, and Mechanistic Crossovers. *J. Am. Chem. Soc.* **2019**, *141*, 9719–9730. [CrossRef]
4. Stamenković, N.; Ulrih, N.P.; Cerkovnik, J. An Analysis of Electrophilic Aromatic Substitution: A "Complex Approach". *Phys. Chem. Chem. Phys.* **2021**, *23*, 5051–5068. [CrossRef]
5. Ingold, C.K. *Structure and Mechanism in Organic Chemistry*, 2nd ed.; Cornell Univ. Press: Ithaca, NY, USA, 1986.
6. Lowry, T.H.; Richardson, K.S. *Mechanism and Theory in Organic Chemistry*; Harper & Row: New York, NY, USA, 1981.
7. Schofield, K. *Aromatic Nitration*; Cambridge University Press: Cambridge, MA, USA, 1980.
8. Kroflič, A.; Huš, M.; Grilc, M.; Grgíc, I. Underappreciated and Complex Role of Nitrous Acid in Aromatic Nitration under Mild Environmental Conditions: The Case of Activated Methoxyphenols. *Environ. Sci. Technol.* **2018**, *52*, 13756–13765. [CrossRef] [PubMed]
9. Coombes, R.G.; Moodie, R.B.; Schofield, K. Electrophilic Aromatic Substitution. Part I. The Nitration Of Some Reactive Aromatic Compounds In Concentrated Sulphuric And Perchloric Acids. *J. Chem. Soc. B* **1968**, 800–804. [CrossRef]
10. Olah, G.A. Aromatic Substitution. XXVIII. Mechanism of Electrophilic Aromatic Substitutions. *Acc. Chem. Res.* **1971**, *4*, 240–248. [CrossRef]
11. Tolgyesi, W.S. Relative Reactivity of Toluene-Benzene in Nitronium Tetrafluoroborate Nitration: Limitation of the Competitive Method of Rate Determination In Fast Reactions. *Can. J. Chem.* **1965**, *43*, 343–355. [CrossRef]
12. Olah, G.A.; Overchuk, N.A. Remarks on the Nitronium Salt Nitration of Toluene and Benzene. *Can. J. Chem.* **1965**, *43*, 3279–3293. [CrossRef]
13. Stock, L.M. *Progress in Physical Organic Chemistry*; Wiley-Interscience: New York, NY, USA, 1976.
14. Ridd, J.H. Mechanism of Aromatic Nitration. *Acc. Chem. Res.* **1971**, *4*, 248–253. [CrossRef]
15. Olah, G.A.; Narang, S.C.; Olah, J.A.; Lammertsma, K. Recent Aspects of Nitration: New Preparative Methods and Mechanistic Studies (A Review). *Proc. Natl. Acad. Sci. USA* **1982**, *79*, 4487–4494. [CrossRef]
16. Brown, R.D. Charge-Transfer Complexes and the Mechanism of Aromatic Substitution. Part I. General Theory. *J. Chem. Soc.* **1959**, 2224–2232. [CrossRef]
17. Fukuzumi, S.; Kochi, J.K. Electrophilic Aromatic Substitution. Charge-Transfer Excited States and the Nature of the Activated Complex. *J. Am. Chem. Soc.* **1981**, *103*, 7240–7252. [CrossRef]
18. Perrin, C.L. Necessity of Electron Transfer and a Radical Pair in the Nitration of Reactive Aromatics. *J. Am. Chem. Soc.* **1977**, *99*, 5516–5518. [CrossRef]
19. Ausloos, P.; Lias, S.G. Reactions of NO_2^+ and Solvated NO_2^+ Ions with Aromatic Compounds and Alkanes. *Int. J. Chem. Kinet.* **1978**, *10*, 657–667. [CrossRef]
20. Bursey, M.M.; Benezra, S.A.; Hoffman, M.K. Electrophilic Aromatic Substitution Reactions. An Ion Cyclotron Resonance Study. *J. Am. Chem. Soc.* **1970**, *92*, 7501–7502. [CrossRef]
21. Hoffman, M.K.; Bursey, M.M. The Structure of the Molecular Ion of C_7H_8 Isomers: An ICR Study. *Tetrahedron Lett.* **1971**, *12*, 2539–2542. [CrossRef]
22. Morrison, J.D.; Stanney, K.; Tedder, J.M. The Reactions of Some Common Electrophiles, CH_3^+, NO^+, NO_2^+, and $O_2NCH_2^+$, with Monosubstituted Benzenes in the Gas Phase. *J. Chem. Soc. Perkin Trans. 2* **1981**, 967–969. [CrossRef]
23. Reents, W.D.; Freiser, B.S. Gas-Phase Nitrosation of Benzene. Implications for Solution Electrophilic Aromatic Substitution Reactions. *J. Am. Chem. Soc.* **1980**, *102*, 271–276. [CrossRef]
24. Attina, M.; Cacace, F.; Yanez, M. Electrophilic aromatic nitration in the gas phase. *J. Am. Chem. Soc.* **1987**, *109*, 5092–5097. [CrossRef]
25. Kenner, J. Oxidation and Reduction in Chemistry. *Nature* **1945**, *156*, 369–370. [CrossRef]
26. Weiss, J. Simple Electron Transfer Processes in Systems of Conjugated Double Bonds. *Trans. Faraday Soc.* **1946**, *42*, 116–121. [CrossRef]

27. Nagakura, S.; Tanaka, J. On the Relation between the Chemical Reactivity and Energy Levels of the Chemical Reagent. *J. Chem. Phys.* **1954**, *22*, 563. [CrossRef]
28. Eberson, L.; Jönsson, L.; Radner, F. Nitration of Aromatics via Electron Transfer; the Relevancy of Experiments Involving Generation of Naphthalene Radical Cation in the Presence of Nitrogen Dioxide. *Acta Chem. Scand. B* **1978**, 32, 749–753. [CrossRef]
29. Rosokha, S.V.; Kochi, J.K. The Preorganization Step in Organic Reaction Mechanisms. Charge-Transfer Complexes as Precursors to Electrophilic Aromatic Substitutions. *J. Org. Chem.* **2002**, *67*, 1727–1737. [CrossRef] [PubMed]
30. Rosokha, S.V.; Kochi, J.K. Strong Electronic Coupling in Intermolecular (Charge-Transfer) Complexes. Mechanistic Relevance to Thermal and Optical Electron Transfer from Aromatic Donors. *New J. Chem.* **2002**, *26*, 851–860. [CrossRef]
31. Kochi, J.K. Inner-Sphere Electron Transfer in Organic Chemistry. Relevance to Electrophilic Aromatic Nitration. *Acc. Chem. Res.* **1992**, *25*, 39–47. [CrossRef]
32. Andrews, L.J.; Keefer, R.M. *Molecular Complexes in Organic Chemistry*; Holden-Day Press: San Francisco, CA, USA, 1964.
33. Foster, R. *Organic Charge-Transfer Complexes*; Academic Press: New York, NY, USA, 1969.
34. Sankararaman, S.; Kochi, J.K. Charge-Transfer Nitration of Naphthalene and the Methylnaphthalenes. Part 1. Direct Comparison with Electrophilic Aromatic Nitrations. *J. Chem. Soc. Perkin Trans.* **1991**, *2*, 1–12. [CrossRef]
35. Masnovi, J.M.; Kochi, J.K.; Hilinski, E.F.; Rentzepis, P.M. Reactive Ion Pairs from the Charge-Transfer Excitation of Electron Donor-Acceptor Complexes. *J. Am. Chem. Soc.* **1986**, *108*, 1126–1135. [CrossRef]
36. Hartshorn, S.R. Non-Conventional Electrophilic Aromatic Substitutions and Related Reactions. *Chem. Soc. Rev.* **1974**, *3*, 167–192. [CrossRef]
37. Queiroz, J.F.; Walkimar, J.; Carneiro, M.; Sabino, A.A.; Sparrapan, R.; Eberlin, M.N.; Esteves, P.M. Electrophilic Aromatic Nitration: Understanding Its Mechanism and Substituent Effects. *J. Org. Chem.* **2006**, *71*, 6192–6203. [CrossRef] [PubMed]
38. Dunbar, R.C.; Shen, J.; Olah, G.A. Substituent Effects in Gas-Phase Ionic Nitration and Acetylation of Aromatics. *J. Am. Chem. Soc.* **1972**, *94*, 6862–6864. [CrossRef]
39. Lu, L.; Liu, H.; Hua, R. HNO_3/HFIP: A Nitrating System for Arenes with Direct Observation of π-Complex Intermediates. *Org. Lett.* **2018**, *20*, 3197–3201. [CrossRef]
40. Feng, J.; Zheng, X.; Zerner, M.C. Theoretical Study of Ipso Attack in Aromatic Nitration. *J. Org. Chem.* **1986**, *51*, 4531–4536. [CrossRef]
41. Politzer, P.; Jayasuriya, K.; Sjoberg, P.; Laurence, P.R. Properties of Some Possible Intermediate Stages in the Nitration of Benzene and Toluene. *J. Am. Chem. Soc.* **1985**, *107*, 1174–1177. [CrossRef]
42. Szabo, K.J.; Hoernfeldt, A.B.; Gronowitz, S. Theoretical Study on Mechanism and Selectivity of Electrophilic Aromatic Nitration. *J. Am. Chem. Soc.* **1992**, *114*, 6827–6834. [CrossRef]
43. Dewar, M.J.S.; Storchb, D.M. Anionic Substitution at Carbonyl Carbon. Implications for the Chemistry of Ions in Solution. *J. Chem. Soc. Perkin Trans. 2* **1989**, 877–885. [CrossRef]
44. Peluso, A.; Del Re, G. On the Occurrence of an Electron-Transfer Step in Aromatic Nitration. *J. Phys. Chem.* **1996**, *100*, 5303–5309. [CrossRef]
45. Albunia, A.R.; Borrelli, R.; Peluso, A. The Occurrence of Electron Transfer in Aromatic Nitration: Dynamical Aspects. *Theor. Chem. Acc.* **2000**, *104*, 218–222. [CrossRef]
46. Herschbach, D.R. Reactive Scattering in Molecular Beams. In *Advances in Chemical Physics*; John Wiley & Sons, Ltd.: Hoboken, NJ, USA, 1966; pp. 319–393.
47. Esteves, P.M.; de M. Carneiro, J.W.; Cardoso, S.P.; Barbosa, A.G.H.; Laali, K.K.; Rasul, G.; Prakash, G.K.S.; Olah, G.A. Unified Mechanistic Concept of Electrophilic Aromatic Nitration: Convergence of Computational Results and Experimental Data. *J. Am. Chem. Soc.* **2003**, *125*, 4836–4849. [CrossRef] [PubMed]
48. Gwaltney, S.R.; Rosokha, S.V.; Head-Gordon, M.; Kochi, J.K. Charge-Transfer Mechanism for Electrophilic Aromatic Nitration and Nitrosation via the Convergence of (ab Initio) Molecular-Orbital and Marcus-Hush Theories with Experiments. *J. Am. Chem. Soc.* **2003**, *125*, 3273–3283. [CrossRef]
49. Marcus, R.A.; Sutin, N. Electron Transfers in Chemistry and Biology. *Biochim. Biophys. Acta* **1985**, *811*, 265–322. [CrossRef]
50. Homogeneous and Heterogeneous Optical and Thermal Electron Transfer. *Electrochim. Acta* **1968**, *13*, 1005–1023. [CrossRef]
51. Xu, X.F.; Zilberg, S.; Haas, Y. Electrophilic Aromatic Substitution: The Role of Electronically Excited States. *J. Phys. Chem. A* **2010**, *114*, 4924–4933. [CrossRef] [PubMed]
52. Shopsowitz, K.; Lelj, F.; MacLachlan, M.J. Regioselectivity in the Nitration of Dialkoxybenzenes. *J. Org. Chem.* **2011**, *76*, 1285–1294. [CrossRef]
53. Parker, V.D.; Kar, T.; Bethell, D. The Polar Mechanism for the Nitration of Benzene with Nitronium Ion: Ab Initio Structures of Intermediates and Transition States. *J. Org. Chem.* **2013**, *78*, 9522–9525. [CrossRef]
54. Koleva, G.; Galabov, B.; Hadjieva, B.; Schaefer III, H.F.; Schleyer, P.v.R. An Experimentally Established Key Intermediate in Benzene Nitration with Mixed Acid. *Angew. Chem. Int. Ed.* **2015**, *54*, 14123–14127. [CrossRef] [PubMed]
55. Nieves-Quinones, Y.; Singleton, D.A. Dynamics and the Regiochemistry of Nitration of Toluene. *J. Am. Chem. Soc.* **2016**, *138*, 15167–15176. [CrossRef] [PubMed]
56. Vidal, M.L.; Epshtein, M.; Scutelnic, V.; Yang, Z.; Xue, T.; Leone, S.R.; Krylov, A.I.; Coriani, S. Interplay of Open-Shell Spin-Coupling and Jahn-Teller Distortion in Benzene Radical Cation Probed by X-ray Spectroscopy. *J. Phys. Chem. A* **2020**, *124*, 9532–9541. [CrossRef]

57. Raghavachari, K.; Haddon, R.C.; Miller, T.A.; Bondybey, V.E. Theoretical Study of Jahn-Teller Distortions in $C_6H_6^+$ and $C_6F_6^+$. *J. Chem. Phys.* **1983**, *79*, 1387–1395. [CrossRef]
58. Takeshita, K. A Theoretical Study on the First Ionic State of Benzene with Analysis of Vibrational Structure of the Photoelectron Spectrum. *J. Chem. Phys.* **1994**, *101*, 2192–2197. [CrossRef]
59. Deleuze, M.S.; Claes, L.; Kryachko, E.S.; François, J.P. Benchmark Theoretical Study of the Ionization Threshold of Benzene and Oligoacenes. *J. Chem. Phys.* **2003**, *119*, 3106–3119. [CrossRef]
60. Haber, K.S.; Zwanziger, F.X.; Campos, R.T.; Wiedmann, R.T.; Grant, E.R. Direct Determination of the Adiabatic Ionization Potential of NO_2 by Multiresonant Optical Absorption. *Chem. Phys. Lett.* **1988**, *144*, 58. [CrossRef]
61. Nemeth, G.I.; Selzle, H.L.; Schlag, E.W. Magnetic ZEKE Experiments with Mass Analysis. *Chem. Phys. Lett.* **1993**, *215*, 151–155. [CrossRef]
62. Lu, K.T.; Eiden, G.C.; Weisshaar, J.C. Toluene Cation: Nearly Free Rotation of the Methyl Group. *J. Phys. Chem.* **1992**, *96*, 9742–9748. [CrossRef]
63. Chai, J.D.; Head-Gordon, M. Long-Range Corrected Hybrid Density Functionals with Damped Atom-Atom Dispersion Corrections. *Phys. Chem. Chem. Phys.* **2008**, *10*, 6615–6620. [CrossRef] [PubMed]
64. Zheng, J.; Xu, X.; Truhlar, D.G. Minimally Augmented Karlsruhe Basis Sets. *Theor. Chem. Acc.* **2011**, *128*, 295–305. [CrossRef]
65. Capobianco, A.; Velardo, A.; Peluso, A. Single-Stranded DNA Oligonucleotides Retain Rise Coordinates Characteristic of Double Helices. *J. Phys. Chem. B* **2018**, *122*, 7978–7989. [CrossRef]
66. Seeger, R.; Pople, J.A. Self-Consistent Molecular Orbital Methods. XVIII. Constraints and Stability in Hartree-Fock Theory. *J. Chem. Phys.* **1977**, *66*, 3045–3050. [CrossRef]
67. Bauernschmitt, R.; Ahlrichs, R. Stability Analysis for Solutions of the Closed Shell Kohn-Sham Equation. *J. Chem. Phys.* **1996**, *104*, 9047–9052. [CrossRef]
68. Marenich, A.V.; Jerome, S.V.; Cramer, C.J.; Truhlar, D.G. Charge Model 5: An Extension of Hirshfeld Population Analysis for the Accurate Description of Molecular Interactions in Gaseous and Condensed Phases. *J. Chem. Theory Comput.* **2012**, *8*, 527–541. [CrossRef]
69. Besler, B.H.; Merz, K.M., Jr.; Kollman, P.A. Atomic Charges Derived from Semiempirical Methods. *J. Comput. Chem.* **1990**, *11*, 431–439. [CrossRef]
70. Reed, A.E.; Curtiss, L.A.; Weinhold, F. Intermolecular Interactions from a Natural Bond Orbital, Donor-Acceptor Viewpoint. *Chem. Rev.* **1988**, *88*, 899–926. [CrossRef]
71. Tomasi, J.; Mennucci, B.; Cammi, R. Quantum Mechanical Continuum Solvation Models. *Chem. Rev.* **2005**, *105*, 2999–3093. [CrossRef] [PubMed]
72. Frisch, M.J.; Trucks, G.W.; Schlegel, H.B.; Scuseria, G.E.; Robb, M.A.; Cheeseman, J.R.; Scalmani, G.; Barone, V.; Petersson, G.A.; Nakatsuji, H.; et al. *Gaussian 16 Revision C.01*; Gaussian Inc.: Wallingford, CT, USA, 2016.